AMERICAN SOCIETY FOR MICROBIOLOGY | Molecular and Cellular Biology

A GIPC1-Palmitate Switch Modulates Dopamine Drd3 Receptor Trafficking and Signaling

Margarita Arango-Lievano,[a,b,c] Ozge Sensoy,[d] Amélie Borie,[a,b,c] Maithé Corbani,[a,b,c] Gilles Guillon,[a,b,c] Pierre Sokoloff,[e]* Harel Weinstein,[f] Freddy Jeanneteau[a,b,c]

Inserm, U1191, Institute of Functional Genomics, Montpellier, France[a]; CNRS, UMR-5203, Montpellier, France[b]; Université de Montpellier, Montpellier, France[c]; Istanbul Medipol University, School of Engineering and Natural Sciences, Istanbul, Turkey[d]; Unit of Neurobiology and Molecular Pharmacology, INSERM U573, Centre Paul Broca, Paris, France[e]; Department of Physiology and Biophysics, Weill Medical College of Cornell University, New York, New York, USA[f]

Palmitoylation is involved in several neuropsychiatric and movement disorders for which a dysfunctional signaling of the dopamine D3 receptor (Drd3) is hypothesized. Computational modeling of Drd3's homologue, Drd2, has shed some light on the putative role of palmitoylation as a reversible switch for dopaminergic receptor signaling. Drd3 is presumed to be palmitoylated, based on sequence homology with Drd2, but the functional attributes afforded by Drd3 palmitoylation have not been studied. Since these receptors are major targets of antipsychotic and anti-Parkinsonian drugs, a better characterization of Drd3 signaling and posttranslational modifications, like palmitoylation, may improve the prospects for drug development. Using molecular dynamics simulations, we evaluated *in silico* how Drd3 palmitoylation could elicit significant remodeling of the C-terminal cytoplasmic domain to expose docking sites for signaling proteins. We tested this model *in cellulo* by using the interaction of Drd3 with the G-alpha interacting protein (GAIP) C terminus 1 (GIPC1) as a template. From a series of biochemical studies, live imaging, and analyses of mutant proteins, we propose that Drd3 palmitoylation acts as a molecular switch for Drd3-biased signaling via a GIPC1-dependent route, which is likely to affect the mode of action of antipsychotic drugs.

The C terminus of G-protein-coupled receptors (GPCRs) has been reported to take part in a large repertoire of protein-protein interactions and represents a functional component of GPCR signaling that is characterized by the malleability of the interface it provides (1, 2). In addition, the GPCR C termini can switch between a soluble form in the cytoplasm and an acylated form anchored to the membrane (3). Among the latter, the palmitoylated form is established by the covalent linkage of a palmitic acid moiety through a thioester bound on one or more cysteine residues often localized in proximity to the conserved amphipathic helical motif 8 (helix-8) (4). The palmitate moiety is thought to be captured in cholesterol-rich membrane environments in order to stabilize GPCRs (5, 6). The helix-8 may adopt a helical structure in the presence of membranes, thereby affecting structural docking sites involved in GPCR dimerization and signaling (7–10). Various suggestions have been offered in the literature regarding the possible regulation of cellular processes by a palmitoylation-dependent conformational switch of the helix-8 in GPCR C-terminal tails. These include G-protein coupling (11), oligomerization (12, 13), regulation of activation (14), receptor turnover (15), and trafficking (16).

Dopamine receptors Drd1 and Drd2 are palmitoylated on one or more cysteine residues within the C-terminal domains, and mutations involving these cysteines result in functional impairment of dopamine signaling (3, 17, 18). However, the molecular mechanisms by which palmitoylation contributes to these effects are not understood. Recent structural modeling of Drd2 helix-8 *in silico*, based on the X-ray structures of Drd3 (19), suggested a putative role for palmitoylation in the anchoring of the Drd2 C terminus into the membrane environment, thus masking some of its molecular motifs (10). In turn, depalmitoylation was hypothesized by molecular modeling to expose the Drd2 C terminus to the aqueous environment, thereby opening possibilities for protein-protein interactions with cytoplasmic partners (10). One illustrative example is the interaction of GIPC1 with the Drd2 C terminus through a region that overlaps with the palmitoylation site (Fig. 1A) (18, 20, 21). Computational modeling of the Drd2-GIPC1 interaction based on the X-ray structures of Drd3 and the PDZ domain of GIPC2 predicted that Drd2 C-terminal palmitoylation could be inhibitory (10), but this has not been tested experimentally. This is all the more intriguing, as the process could be dynamic, catalyzed by palmitoyl transferases and inhibited by thioesterases (22). Because palmitoylation activity was previously mapped in several subcellular compartments, like the biosynthetic pathway (23) and at the plasma membrane of cells in culture (24), cycles of Drd2 palmitoylation-depalmitoylation between subcellular compartments could bias the Drd2-GIPC1 interaction and subsequent signaling.

The interest in signaling modulation by various structural components of GPCRs is related to the growing importance of biased signaling in new drug development. Drd2 and Drd3 are

Received 2 October 2015 **Returned for modification** 27 October 2015
Accepted 6 January 2016

Accepted manuscript posted online 19 January 2016

Citation Arango-Lievano M, Sensoy O, Borie A, Corbani M, Guillon G, Sokoloff P, Weinstein H, Jeanneteau F. 2016. A GIPC1-palmitate switch modulates dopamine Drd3 receptor trafficking and signaling. Mol Cell Biol 36:1019–1031. doi:10.1128/MCB.00916-15.

Address correspondence to Freddy Jeanneteau, freddy.jeanneteau@igf.cnrs.fr.

* Present address: Pierre Sokoloff, PSAdvice, Belleserre, France.

The Unit of Neurobiology and Molecular Pharmacology, INSERM U573 research unit, no longer exists and has been integrated into INSERM UMR894, Center for Psychiatry and Neuroscience, Paris, France.

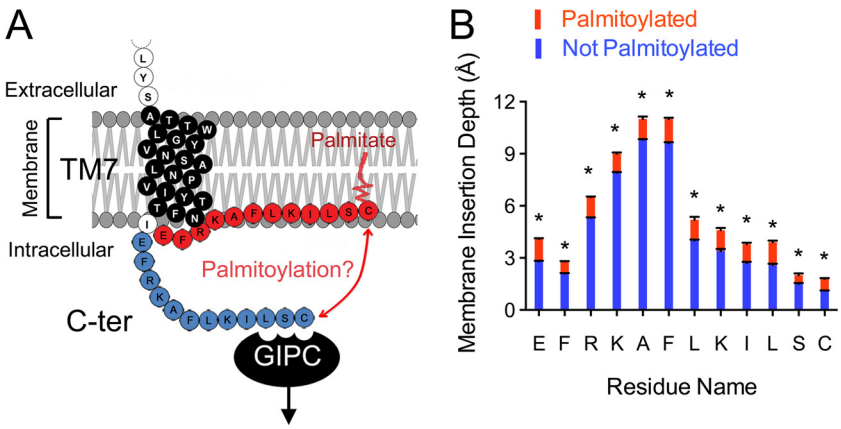

FIG 1 Membrane insertion profile of the (non)palmitoylated Drd3 C terminus. (A) The binding site of GIPC1 to the C-terminal domain of Drd3 contains a putative palmitoylation site. (B) Average backbone insertion values (means ± SEM of 8 replicates) for (non)palmitoylated Drd3 C termini were calculated as described in Materials and Methods. The data show the level of the phosphorous atom of lipids at the water-membrane interface. The model predicted that the Drd3 C terminus is inserted more deeply in the membrane environment when palmitoylated (paired *t* test; *, $P < 0.0001$).

prime targets of antipsychotic and anti-Parkinsonian drugs (25, 26, 27–31). The two dopamine receptor subtypes share common signaling cascades, including inhibition of cyclic AMP (cAMP) formation through G_i/G_O coupling and phospholipase C, regulation of ion channel activities, and stimulation of mitogenesis through the activation of mitogen-activated protein kinases and Akt (32–35). The close homology between Drd2 and Drd3 suggests that C-terminal palmitoylation could be a common mechanism for controlling signaling via the helix-8. To explore this hypothesis, we undertook *in silico* and *in cellulo* analyses of the impact of palmitoylation on Drd3 signaling via GIPC1, an interacting protein (21).

GIPC1 has previously been identified as an interacting protein for several transmembrane and membrane-associated proteins, including but not limited to GAIP, a regulator of G protein signaling (36), β1-adrenergic receptors (37), semaphorin M-SemF (38), glucose transporter GLUT1 (39), tyrosine kinase receptors like the neurotrophin receptors tropomyosin-related kinases (TrkA and TrkB) (40), insulin-like growth factor 1 (IGF-1) receptor (41), transforming growth factor β (TGF-β) receptor type III (42), and lysophosphatidic acid receptor 1 (LPA1) (43). These studies suggested a possible role for GIPC1 in the regulation of vesicular trafficking (36, 40, 43), receptor surface expression (39, 42), and G protein signaling (36, 37, 40, 41). In the case of Drd2 and Drd3, dopamine signaling via the cAMP route is negatively regulated by GIPC1 by way of a direct interaction with the PDZ (PSD95/Dig/ZO-1) and the acyl carrier protein (ACP) domains (21). Previous studies implicated other ACP domains in the transfer of acyl coenzyme A (acyl-CoA) moieties, including palmitoyl-CoA, to the catalytic domain of acyl transferases and thioesterases (44–46). The questions remain whether Drd3 is indeed palmitoylated and if the presence of the ACP domain provides GIPC1 with regulatory functions. The Drd3 C terminus consists of a conserved amphipathic helical motif (Hx8) that contains the Lys-Ser-Cys motif for GIPC1 binding and a putative C-terminal palmitoylation site (Fig. 1A). The two sites overlap, suggesting the possibility of competitive interaction between GIPC1 binding and palmitoylation.

MATERIALS AND METHODS

Computational modeling. The computational modeling of the dynamic behavior of Helix-8 of Drd3 in a membrane system was performed as previously described for Drd2 (10). A series of coarse-grained MD simulations (CGMD) was carried out for a system composed of the transmembrane 7 (TM7)–helix-8 segment from Drd3. The CGMD simulations were done with the Martini force field, following established protocols (47–49). Briefly, an integration step of 0.04 ps was used, and long-range electrostatic and van der Waals interactions were calculated with shift functions. For the latter, we used a twin-range cutoff scheme of 0.9 and 1.2 Å, with the neighboring list updated every 10 ps. The Berendsen algorithm was used to maintain constant temperature and pressure (50). Simulations were performed in a lipid membrane composed of 70% sphingomyelin and 30% cholesterol to mimic lipid rafts that act as membrane microdomains for the assembly of signaling molecules (51, 52). All the systems were neutralized at 0.15 M NaCl (47, 53). The complete simulated system is composed of the Drd3 entire TM7 (residues 372 to 388) together with parts of the extracellular loop 3 (residues 368 to 371) and the entire amphipathic helix-8 (residues 389 to 400) of human Drd3 (hDrd3). The backbone atoms of TM7 were restrained to their initial coordinates to maintain the orientation adopted by TM7 within the membrane in the complete structure of the receptor. The palmitoylated C terminus was obtained by patching the palmitate group to the terminal cysteine residue of helix-8 and was considered to be in the zwitterionic form. The effect of reversible palmitoylation on the depth of membrane penetration of the entire amphipathic helix-8 in this segment was evaluated. Simulations of (non)palmitoylated Hx8 were performed for 4 μs (effective time). To determine convergence, the backbone insertion depth of each residue of helix-8 was monitored between successive predetermined lengths of windows over the entire trajectory; 100-ns windows were used. A cutoff of 0.05 Å was used as the convergence criterion between subsequent windows. The depth of insertion of the helix-8 backbone was calculated by including the nitrogen, Cα atom, and the carbonyl group. The average insertion was determined with respect to the phosphorous atoms of the membrane lipid headgroups present within a 2-Å cutoff distance from the backbone of helix-8.

Plasmids. The human Drd3 was tagged at the N terminus with the enhanced green fluorescent protein (GFP) fused to the nicotinic receptor α7 subunit signal peptide (54) using the pCEP4 vector (Invitrogen Corp.). The GFP-Drd3ΔC receptor mutant was previously described (21), the GFP-Drd3CS mutant was generated by site-directed mutagenesis with QuikChange kit (Agilent Technologies), and GFP-Drd3/β2AR was generated by PCR using the following oligonucleotides (underlined sequences specify restriction sites for cloning): sense, 5′-CCCAAGCTTGGAAGGCGGGGCAG-3′, and antisense 5′-GCTCTAGAGCTCGAGTCATAGTAGCGATCTTCTGAGGCAGCAGCAGGACAGGATCTTGAGGAAGG-3′. C-terminal domains of Drd3 (animo acids 389 to 400) and mu-

tants (Drd3ΔC and Drd3/β2AR) were inserted in frame downstream of the B42 activation domain into a pEG202 vector and GIPC1 subcloned into pJG4.5 downstream of the LexA domain to perform the 2-hybrid binary complementation assay (OriGene Technologies, Rockville, MD) as previously described (21). GIPC1 and a mutant lacking the ACP domain (ΔACP, lacking amino acids 223 to 316) were constructed by PCR and subcloned into the pcDNA3.1HisC vector (Invitrogen Corp., San Diego, CA). The resulting GIPC1 contained a dual 6×His/Xpress tag at the N terminus. All constructs were verified by automated nucleotide sequencing (Licor, Lincoln, NE).

Reagents. Dopamine, ascorbic acid, hydroxylamine, *N*-ethylmaleimide, palmitic acid, and 2-bromohexadecanoic acid (2BrP) were obtained from Sigma. Commercial antibodies were as follows: anti-extracellular signal-regulated kinases 1 and 2 (anti-ERK1/2; catalog number M3807; Sigma) and the phospho-ERK1/2[T202/Y204] (catalog number 9101), phosphor-AKT[S473] (catalog number 9271), and AKT (catalog number 9272) antibodies were from Cell Signaling Technologies. The 6×His tag and streptavidin-horseradish peroxidase (HRP) were from ThermoScientific. GFP antibodies (catalog number Ab13970) were from Abcam. Homemade antibodies against GIPC1 and Drd3 were previously described (21, 55).

Cell culture and transfections. HEK293 cells and CHO cells were cultured in Dulbecco's modified Eagle's medium (DMEM; Life Technologies, Rockville, MD) supplemented with 10% fetal calf serum and 100 μg/ml penicillin-streptomycin in a humidified atmosphere of 5% CO_2, 95% air. Striatal primary neuron cultures derived from time-pregnant Sprague-Dawley rat (Janvier Lab) embryos at day 18 (E18) were prepared on glass coverslips coated with poly-D-lysine (0.1 μg/ml) and grown for 3 weeks in neurobasal medium supplemented with B27 (Invitrogen) with a 1/10 proportion of cortical neurons. The protocol complied with the European Communities Council Directive (86/609/EEC) and was approved by the Ministère de la Recherche Française (agreement number CEEA-LR-00651.01). Transfections were performed with Lipofectamine 2000 (Life Technologies, Rockville, MD). Palmitic acid and 2-bromo-palmitate (Sigma) were prepared fresh as stock solutions in ethanol (EtOH; 3% final concentration) and diluted further with culture medium. The vehicle consisted of 3% EtOH.

[^{3}H]palmitate protein labeling assay. HEK293 cells were starved from serum for 1 h prior to the addition of 0.4 mCi/ml de-[^{3}H]palmitate ([9,10-^{3}H]palmitate; 30 to 60 Ci/mmol; NEN) for 50 min. Cells were rinsed several times in phosphate-buffered saline (PBS) before solubilization in a digitonin-cholate lysis buffer (50 mM Na/Na_2PO_4 [pH 7.4], 300 mM NaCl, 4% digitonin, 1% cholate-Na, and protease inhibitors) for 45 min at 4°C. Lysates were diluted with 1 volume of double-distilled water and centrifuged at 50,000 × *g* for 40 min. Supernatant containing the solubilized Drd3 was collected, and the protein concentrations were measured with Coomassie stain (Bio-Rad) and bovine serum albumin (BSA) as the standards. Normalized protein levels were further diluted 20 times with 50 mM Na/Na_2PO_4 (pH 7.4) and cleared with normal rabbit IgG (Santa Cruz Biotechnology) prior to immunoprecipitation of the Drd3 receptors with anti-GFP antibodies (Abcam) overnight and a 2-hour incubation with a 50% slurry of protein A-Sepharose (Amersham Pharmacia Biotech). Beads were rinsed 5 times with the diluted solubilization buffer and suspended in a nonreducing sample loading buffer. Proteins were separated by SDS-PAGE (4 to 12% acrylamide gradient; Life Technologies). Proteins were fixed in the gels by using 10% acetic acid and 40% isopropanol in water and further incubated with 1 M hydroxylamine (pH 7) prior to fluorographic signal amplification (Amplify; Amersham Pharmacia Biotech). Finally, gels were dehydrated and exposed to MP films (Amersham Pharmacia Biotech) for 4 to 8 weeks. Autoradiographic films were digitalized, and signals were measured based on the optical density, using the public domain NIH Image program version 1.63 (developed at the U.S. National Institutes of Health and available on the Internet at http://rsb.info.nih.gov/nih-image/).

Nonradioactive detection of palmitoylation by ABE. Palmitoylation of the GFP-Drd3 and mutant CS expressed transiently in HEK293 cells was assayed using the acyl-biotin exchange (ABE) method as previously described (56, 57). In brief, GFP-Drd3 constructs were immunoprecipitated with GFP antibodies in lysis buffer supplemented with 50 mM *N*-ethylmaleimide to block nonpalmitoylated cysteines. Further treatment with 1 M hydroxylamine cleaved the thioester bonds at palmitoylated cysteines. GFP-Drd3 contructs were treated with thiol-reactive biotin-BMCC (ThermoScientific), and palmitoylated cysteine was further detected with streptavidin-HRP (ThermoScientific) by Western blotting.

[^{125}I]iodosulpride binding assays. Drd3 ligand binding experiments were performed on purified membrane fractions using 0.1 nM [^{125}I]iodosulpride (Amersham Pharmacia Biotech) as previously described (58). To detect Drd3 present at the cell surface, we used the Drd3 ligands dopamine and iodosulpride, which cannot diffuse through membranes. To this end, whole cells were scratched off culture dishes, harvested by centrifugation, suspended in DMEM–F-12 supplemented with ascorbic acid (50 μg/ml), and incubated in quadruplicate for 30 min at 30°C with 0.1 nM [^{125}I]iodosulpride (Amersham Pharmacia) in the increasing concentrations of nonradioactive dopamine. Nonspecific binding was measured in the presence of eticlopride (1 μM). Binding was stopped by filtration through GF/C filters coated with polyethyleneimine (0.3%, vol/vol), and radioactivity was counted on the filter by gamma scintigraphy. Dopamine competition curves were analyzed by nonlinear regression with a two-site model by using Prism software (GraphPad, San Diego, CA). The protein concentration was estimated with the Coomassie protein assay reagent using a wide range of BSA concentrations as standards.

^{125}I-cAMP accumulation assay. Cells were preincubated with 10 μM 3-isobutyl-1 methylxanthine in α-minimal essential medium for 25 min and treated with increasing concentrations of dopamine for 10 min in the presence of 0.5 μM forskolin. The reaction was stopped by addition of 50 μl of ice-cold 0.1 M HCl. Cells were sonicated, and cAMP accumulation was assayed with a ^{125}I-cAMP radioimmunoassay kit (DuPont/NEN, Boston, MA).

Binary two-hybrid protein interactions. Binding of the Drd3 C terminus to GIPC1 was measured with the DupLex-A two-hybrid system kit (OriGene Technologies) in the *Saccharomyces cerevisiae* strain EGY48, which harbors the reporter genes for LEU1 and β-galactosidase under the control of upstream LexA binding sites. Transformants were grown on selective medium and assayed for β-galactosidase (β-Gal) to verify and quantify interactions in a solid support assay and liquid culture assay, respectively, with 5-bromo-4-chloro-3-indolyl-β-D-galactopyranoside (X-Gal) and *o*-nitrophenyl-D-galactopyranoside (ONPG) as substrates, according to the yeast protocols handbook from Clontech (Palo Alto, CA). One unit of β-Gal was defined as the amount that hydrolyzed 1 μmol of ONPG per min per cell.

Endoplasmic reticulum exit assay. Nonpermissive temperature shifts have been previously used to reduce protein trafficking in the secretory pathway and accumulate transmembrane cargo proteins in the pericentriolar intermediate compartment (59). Transfected HEK293 cells were grown at a restrictive temperature of 20°C overnight to block GFP-Drd3 cargo in the pericentriolar endoplasmic reticulum (ER) to the Golgi compartment. Back at a permissive temperature of 37°C, cells started to express GFP-Drd3 at the plasma membrane. Cycloheximide (CHX) was added to cells for at least 1 h prior to temperature shift (from 20°C to 37°C) to prevent the synthesis of new GFP-Drd3 cargo and follow the ER exit of the existing pool of GFP-Drd3 cargo. Therefore, the thermal shift ER exit assay combined with CHX permitted the analysis of GFP-Drd3 targeting to the plasma membrane as a function of GIPC1 overexpression and palmitoylation in cell preparations fixed with ice-cold 2% paraformaldehyde (PFA).

Immunolabeling. Cells were grown on collagen-coated coverslips and fixed in 2% paraformaldehyde–PBS (pH 7.4) for 20 min at room temperature, washed twice in PBS-glycine buffer (0.1 M, pH 7.4), and permeated

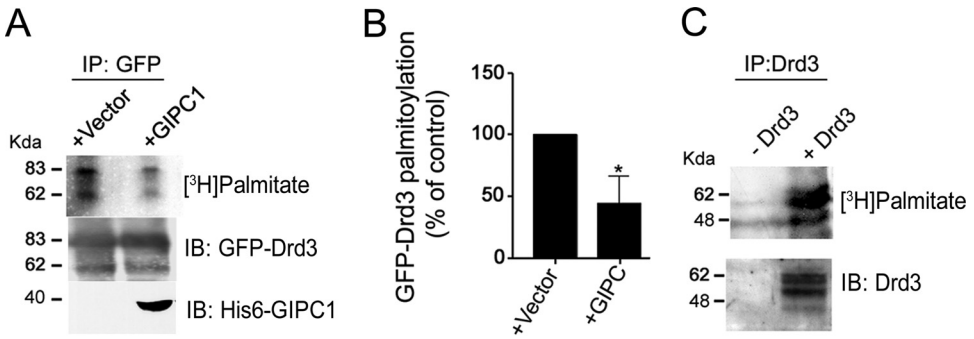

FIG 2 Drd3 palmitoylation and effect of GIPC1. (A) Incorporation of [^{3}H]palmitate in HEK293 cells transiently transfected with GFP-Drd3 and His6-GIPC1. Results of fluorography of immunopurified GFP-Drd3 using anti-GFP antibodies are shown. (B) Means ± SEM collected from 4 independent experiments (unpaired *t* test; $P < 0.05$). (C) Incorporation of [^{3}H]palmitate in Drd3 stably expressed in CHO cells. Fluorography results are show for the radioactivity incorporated into Drd3 and for Western blotting of Drd3 protein immunopurified from cell lysates with specific antibodies against Drd3.

for 20 min with 0.05% saponin while blocking in 10% fetal bovine serum–PBS. GIPC1 was labeled with an anti-Xpress antibody (1:3,000 dilution; Life Technologies), and Drd3 was labeled with a GFP antibody (1:3,000 dilution; Abcam) in incubation buffer (0.1% BSA–PBS supplemented with 10% fetal bovine serum). A-LexA-conjugated secondary antibodies were used for detection (1:1,000 dilution; Molecular Probes). GFP-Drd3 prominently localized to the plasma membrane after treatment with 20 μg/ml CHX for at least 5 h to clear the intracellular biosynthetic pathway. Previously described home-made antibodies were used to stain the endogenous GIPC1 and Drd3 on adult rat brain sections fixed with 4% paraformaldehyde (21). Images were acquired with a laser scanning confocal image system (TCS SPII software; Leica, Deerfield, IL) coupled to a Leica DM R fluorescence microscope. When necessary, fluorescent images were transformed into grayscale pixels, and ImageJ plug-ins were applied to trace the regions of interest (ROI; the plasma membrane and the intracellular compartment).

GFP antibody feeding assay. GFP antibodies were applied in the culture medium of living cells at 4°C for 30 min to limit vesicular transport. This allowed for the labeling of the GFP-Drd3 constructs present at the cell surface under detergent-free conditions with Alexa Fluor 555-conjugated secondary antibodies. ImageJ was utilized to measure the surface covered by Alexa Fluor 555 and GFP signals in the same ROIs of at least 10 cells per condition.

Fluorescence imaging. Time-lapse imaging of transfected GFP-Drd3 in HEK293 cells seeded on poly-D-lysine-coated Ibidi bottom dishes (Biovalley) was performed with an inverted epifluorescence microscope (1X70; Olympus) coupled with a Coolsnap HQ camera (Roper Scientific, France). ImageJ plug-ins were used to align image stacks and track vesicle movement in time series images.

Statistical analysis. For simulation data, the standard error (SE) from 8 replicates was calculated according to the following formula: $SE = \left\{ \sqrt{\frac{\Sigma_{(s=1)}^{m} \Sigma_{(i=1)}^{n} Y_{is}^{2}}{(n_y - 1)(n_y)}} \right\}^{1/2}$, where *s* is the series number, *i* is the point number in series *s*, *m* is the number of series for point *y* in the chart, *n* is the number of points in each series, Y_{is} is the data value for series *s* and the *i*th point, and n_y is the total number of data values in all series. For *in cellulo* data, the averages ± standard errors of at least three independent experiments are presented. For [^{125}I]iodosulpride binding, ^{125}I-cAMP accumulation, and binary 2-hybrid assays, each sample was analyzed in triplicate. Significance ($P < 0.05$) was determined using the two-tailed Student *t* test.

RESULTS

***In silico* simulations show that palmitoylation increases Drd3 C-terminal penetration in the membrane.** We investigated by using computational approaches and a Drd3 three-dimensional model the relationship between palmitoylation and membrane insertion of the Drd3 C terminus by CGMD simulations, as described in detail in the Materials and Methods section. We found that the helix-8 inserted deeper in a membrane composed of 70% to 30% sphingomyelin-cholesterol (Fig. 1B). Palmitoylation statistically increased the overall penetration depth of each residue of the helix-8 residues (Fig. 1B). Therefore, we concluded that the C terminus tail of the Drd3 is more accessible to the aqueous environment when depalmitoylated, raising the possibility that Drd3 palmitoylation and GIPC1 binding are competitive processes.

***In cellulo*, GIPC1 diminished Drd3 palmitoylation.** We monitored Drd3 palmitoylation by using a reconstituted system consisting of HEK293 cells transfected transiently with the human Drd3 construct fused with EGFP at the N terminus to preserve C-terminal motifs and facilitate biochemical and functional studies. Metabolic labeling by incorporation of [^{3}H]palmitate revealed Drd3 palmitoylation after immunoprecipitation with specific GFP antibodies and fluorography (Fig. 2A). To examine the impact of GIPC1, we cotransfected GIPC1 with GFP-Drd3 in HEK293 cells and recapitulated the metabolic labeling with [^{3}H]palmitate followed by fluorography on the GFP immunoprecipitates. We found that GIPC1 decreased GFP-Drd3 palmitoylation (Fig. 2A and B), an effect that did not result from the reduced expression levels of GFP-Drd3. Furthermore, the N-terminal GFP tag did not interfere with either dopamine binding (mean ± SEM for Drd3 of 20.94 ± 1.12 nM, compared to results for GFP-Drd3, 25.61 ± 1.38 nM; $n = 3$ independent experiments) or Drd3 palmitoylation (Fig. 2C) monitored by [^{3}H]palmitate incorporation followed by the immunoprecipitation of Drd3 with a specific antiserum previously described (55).

Palmitoylation diminished Drd3 colocalization with GIPC1. To block palmitoylation *in cellulo*, we used 2-bromopalmitate (2BrP) as a competitive and irreversible general inhibitor of palmitoyl transferases (60, 61). We found that 2BrP inhibited the palmitoylation of GFP-Drd3 when incubated before metabolic labeling with [^{3}H]palmitate (Fig. 3A and B). We then monitored the colocalization of GFP-Drd3 and GIPC1 as a function of cellular palmitoylation. In control cells treated with vehicle, colocalization of GFP-Drd3 with GIPC1 was detected at the plasma membrane and in vesicles (Fig. 3C) as previously described (21). In comparison, cells treated with 2BrP demonstrated colocalization

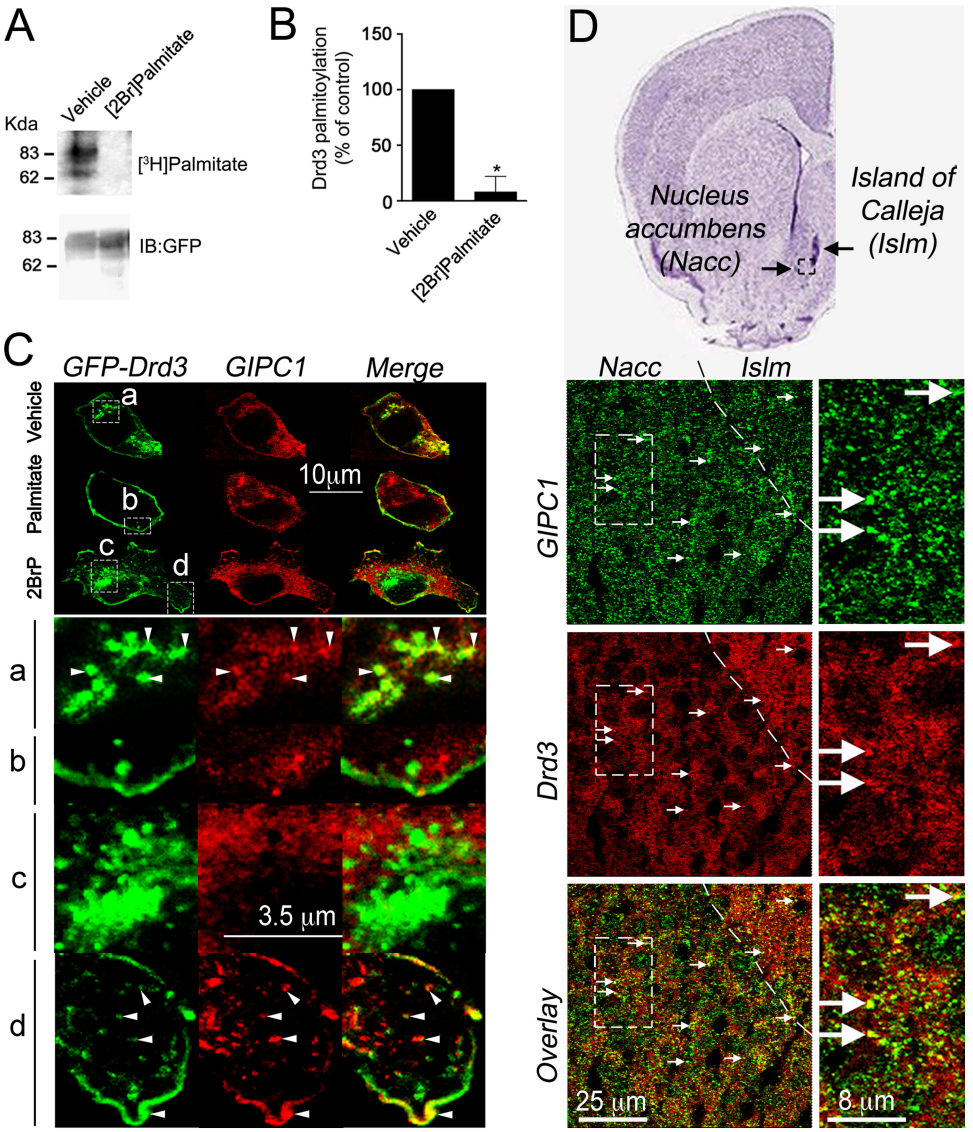

FIG 3 Disruption of Drd3 palmitoylation and colocalization of Drd3 with GIPC1. (A) Pharmacological blockage of GFP-Drd3 palmitoylation with 100 μM 2BrP added overnight prior labeling of transfected HEK293 cells with [^{3}H]palmitate. Fluorography results with immunopurified GFP-Drd3 with GFP antibodies are shown. (B) Means ± SEM of data collected from 3 independent experiments (unpaired *t* test; $P < 0.05$). (C) HEK293 cells cotransfected with GFP-Drd3 and GIPC1 constructs treated with 20 μM palmitate or 20 μM 2BrP overnight. GIPC1 and Drd3 partially colocalized at the plasma membrane and in vesicles of vehicle- and 2BrP-treated cells (insets a and d, respectively). GFP-Drd3 did not colocalize with GIPC1 in palmitate-treated cells (inset b) and in the perinuclear region of 2BrP-treated cells (inset c). (D) Immunolabeling of endogenous GIPC1 and Drd3 in the adult rat brain on a coronal section at +1.2 mm from bregma, as depicted on a Nissl-stained slice (top). Arrows point to colocalization found in the granular cells in the islands of Calleja (Islm) and in medium-sized spiny neurons in the nucleus accumbens (Nacc).

of GFP-Drd3 with GIPC1 at the plasma membrane and vesicles in the proximal region (Fig. 3C, inset d) but not in the pericentriolar region (Fig. 3C, inset c). Finally, cells treated with palmitate demonstrated little colocalization between GIPC1 and GFP-Drd3 (Fig. 3C, inset b). The results indicated that only a subset of GFP-Drd3-containing vesicles colocalized with GIPC1 as a function of palmitoylation in HEK293 cells. Likewise, GFP-Drd3 colocalized, partially, with GIPC1 in the adult rat brain, thus confirming the physiological relevance of the punctate staining observed in HEK293 cells (Fig. 3D).

Alterations of GFP-Drd3 cell surface presentation and signaling by palmitoylation and GIPC1. Inhibition of palmitoylation by 2BrP resulted in the accumulation of GFP-Drd3 in cytoplasmic vesicles of transfected primary medium spiny neurons (MSNs) (Fig. 4A) as well as in transfected HEK293 cells (Fig. 5A). This effect was reproduced by the overexpression of GIPC1 with no additive effects of 2BrP in HEK293 cells (Fig. 5B). Consequently, a deficiency of Drd3 palmitoylation could impinge on the delivery of Drd3 to the cell surface. To test this hypothesis, we monitored Drd3 anterograde targeting in transfected cells grown from a nonpermissive to a permissive temperature. At 20°C, GFP-Drd3 constructs accumulate in the ER and move to the plasma membrane when returned to 37°C (Fig. 5C). The impact of cellular palmitoylation was tested with 2BrP treatment during the per-

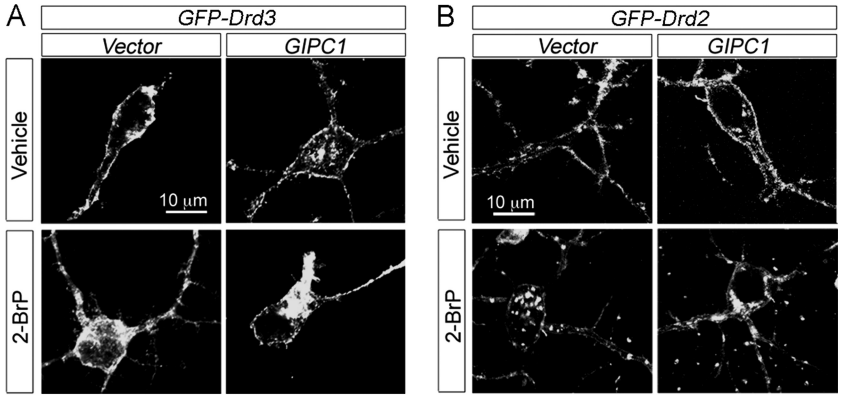

FIG 4 Localization of GFP-Drd2 and GFP-Drd3 in primary medium spiny neurons. Representative distribution of GFP-Drd3 (A) and GFP-Drd2 (B) in rat embryo-derived striatal neurons cotransfected after 3 weeks in culture with the vector or GIPC1 and after treatment with 50 μM 2-BrP overnight.

missive state, and the role of GIPC1 was assessed by transfection from the nonpermissive state onwards. We found that 2BrP and GIPC1 diminished the localization of GFP-Drd3 at the plasma membrane with no additive effects (Fig. 5D). To assess the functional consequence of palmitoylation on Drd3 signaling, we measured the inhibition by dopamine of forskolin (FSK)-stimulated cAMP accumulation, since Drd3 is negatively coupled to this pathway (30, 34). Dopamine inhibited cAMP accumulation by 66% ± 4% in the vector-transfected control cells, and this response was impaired by addition of 2BrP (30% ± 14%; $P = 0.0001$ compared to vehicle). The response to dopamine was less efficient in the presence of GIPC1 (40% ± 6.4%; $P = 0.0068$ compared to vector), and 2BrP had no greater more effect (45% ± 6.6%; $P = 0.608$ compared to GIPC1 plus vehicle) (Fig. 5F).

Additionally, we monitored other Drd3 signaling pathways via the kinases Akt (Fig. 5G) and Erk (Fig. 5H). Dopamine inhibited Akt phosphorylation independently of GIPC1 and 2BrP pretreatment. In contrast, the activation of the Erk pathway by dopamine depended on pretreatment with 2-BrP with no obvious effects of GIPC1. Together, the results indicated that only the cAMP pathway is sensitive to both palmitoylation and GIPC1.

Palmitoylation reduced GFP-Drd3 cargo trafficking. To investigate the role of cellular palmitoylation on Drd3 cellular trafficking, we performed time-lapse microscopy of GFP-Drd3 cargoes in HEK293 cells cotransfected with GIPC1 (Fig. 6A). Control cells treated with vehicle exhibited equal numbers of stationary and trafficking vesicles. Treatment with palmitate increased significantly the proportion of stationary GFP-Drd3-containing vesicles. In contrast, inhibition of cellular palmitoylation with 2BrP increased significantly the proportion of GFP-Drd3 cargoes trafficking. Overall, the proportion of stationary GFP-Drd3 cargoes increased and decreased, respectively, with palmitate and 2BrP treatment (Fig. 6B). The size of a single GFP-Drd3 cargo vesicle was ~0.3 μm, and trafficking velocity was 0.24 ± 0.02 μm/s. Interestingly, the velocity of GFP-Drd3 cargoes did not change with treatments. However, the total distance traveled by cargoes significantly diminished upon treatment with palmitate (2.13 ± 0.58 μm/40 s) compared to 2BrP-treated cells (9.1 ± 0.47 μm/40 s) or vehicle controls (9.63 ± 0.81 μm/40 s). The data are consistent with an increased proportion of stationary cargoes in cells exposed to palmitate, whereas the reverse was observed upon treatment with 2BrP (Fig. 6C).

Role of a GIPC1 mutant that cannot bind to Drd3. Previous *in silico* structural modeling using Drd2 as the template predicted that (i) the GIPC1 PDZ domain alone is not sufficient to bind to the palmitoylated C-terminal PDZ binding motif and that (ii) depalmitoylation of the C-terminal cysteine enables a distancing of the PDZ binding motif away from the membrane environment (10). Given that both the PDZ and ACP domains are required to bind the Drd3 C terminus in a yeast two-hybrid assay (21), we investigated the role of the ACP domain in GFP-Drd3 subcellular distribution and signaling. To this end, we generated a mutant deprived of the ACP domain only (GIPC1ΔACP) (Fig. 7A) and confirmed by coimmunoprecipitation that GIPC1 required the ACP to interact with GFP-Drd3 in HEK293 cells (Fig. 7B). Functionally, transfection of GIPC1ΔACP failed to reduce the cAMP response to dopamine (Fig. 7C) and failed to reduce the presentation of GFP-Drd3 to the plasma membrane (Fig. 7D) compared to wild-type GIPC1. Additionally, 2BrP treatment reduced GFP-Drd3 cell surface presentation in cells transfected with GIPC1ΔACP but not in the cells transfected with GIPC1 (Fig. 7E). Therefore, the ACP domain is required for GIPC1 to recapitulate the effects of 2BrP.

Role of a palmitoylated Drd3 mutant that cannot bind to GIPC1. According to the hypothesis, a deletion mutant lacking the C-terminal cysteine (GFP-Drd3ΔC) should impair both Drd3 palmitoylation and GIPC1 binding (21). To dissociate Drd3 palmitoylation from the interaction of Drd3 with GIPC1, we generated a chimera of Drd3 and β2AR C-terminus tails (GFP-Drd3/β2AR) that preserved the Drd3 palmitoylation site, Leu-Ser-Cys, as an internal motif followed by the C-terminal PDZ binding motif, Ser-Leu-Leu_{COOH} of the β2AR, because it cannot bind to GIPC1 (37). Use of these mutants confirmed two predictions: (i) Drd3ΔC and Drd3/β2AR failed to bind to GIPC1 in a binary two-hybrid assay in yeast (Fig. 8A), and (ii) GFP-Drd3ΔC failed to be palmitoylated, in contrast to GFP-Drd3 and GFP-Drd3/β2AR (Fig. 8B), indicating that the C-terminal cysteine residue is the primary palmitoylation site for Drd3.

Further fluorescence microscopy of transfected cells indicated that GFP-Drd3 and GFP-Drd3/β2AR were distributed mostly at the plasma membrane, compared to GFP-Drd3ΔC, which accumulated in cytoplasmic compartments (Fig. 8C). Whole-cell [^{125}I]iodosulpride binding confirmed that GFP-Drd3ΔC did not efficiently reach the plasma membrane, compared to GFP-Drd3

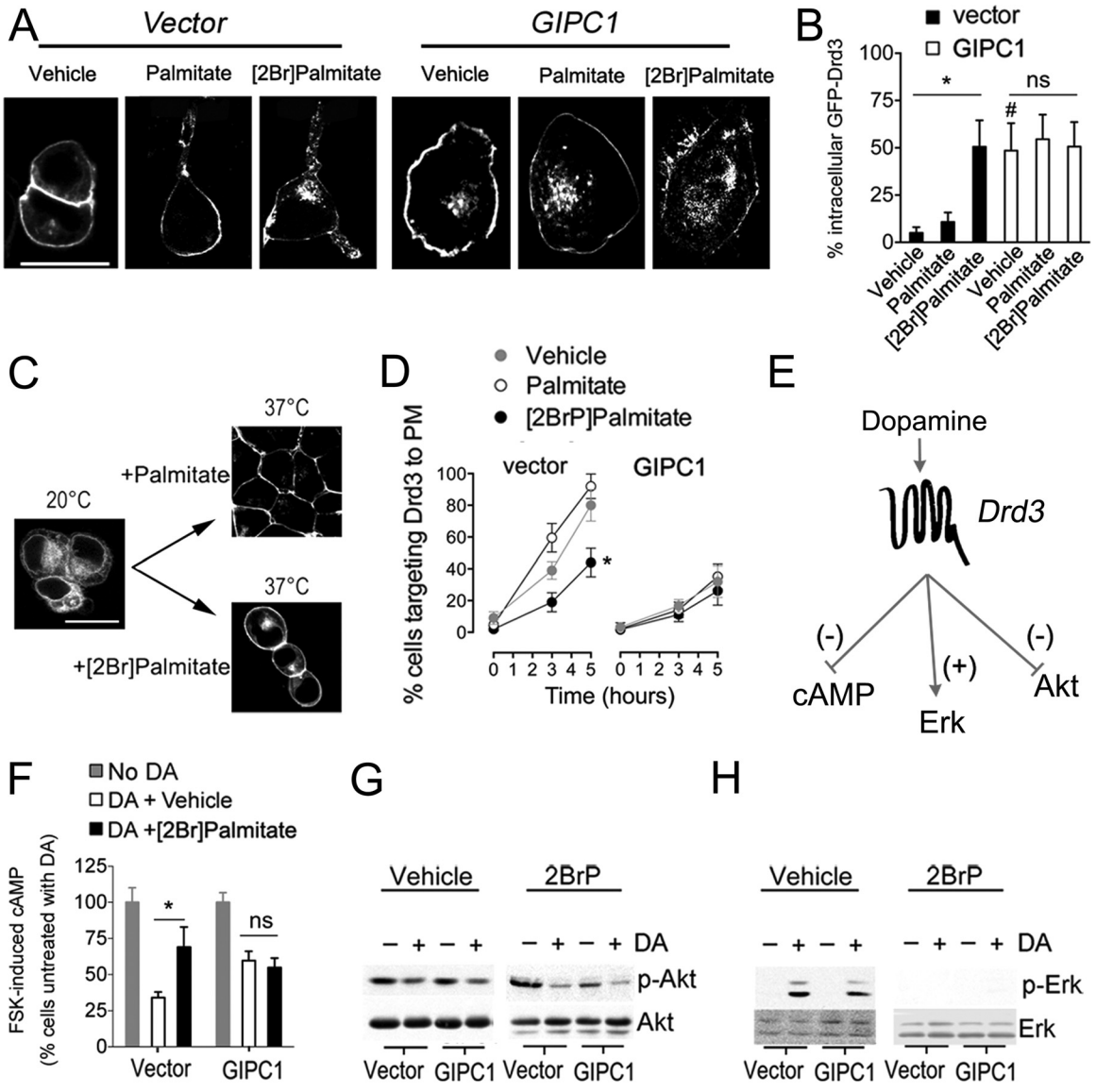

FIG 5 Disruption of palmitoylation with 2BrP impaired GFP-Drd3 functions. (A) Representative images of GFP-Drd3 subcellular distribution in HEK293 cells treated with 100 μM palmitate or 100 μM 2BrP overnight. Bar, 20 μm. (B) Proportion of GFP-Drd3 fluorescence in the cytoplasm of HEK293 cells cotransfected with GIPC1 or with the control vector relative to the total fluorescence (unpaired *t* test: *, $P = 0.033$ for vehicle versus 2-BrP; #, $P = 0.042$ for vector versus GIPC1). (C) Thermal shift to 20°C overnight resulted in the accumulation of transfected GFP-Drd3 in the ER that resolved when cells were returned to 37°C for several hours. The effect of palmitoylation was assessed in the presence of 100 μM 2BrP or 100 μM palmitate. Bar, 15 μm. (D) Means ± SEM of data collected from 3 independent experiments, expressed as the percentage of cells targeting Drd3 to the plasma membrane (PM). Two-way analysis of variance for the interaction of time with palmitoylation on Drd3 presentation at the cell surface [$F_{(4, 18)} = 3.385$; *, $P = 0.0312$) is lost in cells overexpressing GIPC1 ($F_{(4, 18)} = 0.1515$; $P = 0.95$). (E) It is known that Drd3 activation inhibits cAMP formation and Akt phosphorylation and that it activates Erk1/2, but the role of GIPC1 and palmitoylation is unknown. (F) Effect of 15 μM 2-BrP overnight on the inhibition of cAMP accumulation by a 15-min stimulation with 0.1 μM dopamine (DA) in the presence of 0.5 μM FSK in HEK293 cells cotransfected with GFP-Drd3 and GIPC1 or the control vector. Mean ± SEM data were collected from 6 experiments (unpaired *t* test; $P < 0.05$). (G) Effect of 50 μM 2-BrP overnight on the inhibition of Akt phosphorylation by a 4-min stimulation with 0.1 μM DA in HEK293 cells cotransfected with GFP-Drd3 or the control vector or GIPC1. (H) Effect of 50 μM 2-BrP overnight on the phosphorylation of Erk1/2 by a 4-min stimulation with 0.1 μM DA in HEK293 cells cotransfected with GFP-Drd3 and the control vector or GIPC1.

or GFP-Drd3/β2AR (Fig. 8D). Yet, GFP-Drd3ΔC responded to dopamine by activating Erk phosphorylation as a function of 2-BrP pretreatment (Fig. 8E). In contrast, GFP-Drd3ΔC failed to inhibit Akt phosphorylation with or without pretreatment with 2BrP (Fig. 8E). To determine the role of Drd3 palmitoylation independently of GIPC1 binding, we treated GFP-Drd3/β2AR-transfected cells with 2BrP. We found that inhibition of cellular palmitoylation was sufficient to reduce whole-cell [^{125}I]iodosulpride binding to floor levels of the GFP-Drd3 control (Fig. 8F). In contrast, cell surface [^{125}I]iodosulpride binding of the GFP-Drd3ΔC construct was low and independent of 2BrP treatment (Fig. 8F).

Role of a nonpalmitoylated Drd3 mutant that can bind to GIPC1. To determine the role of Drd3 palmitoylation indepen-

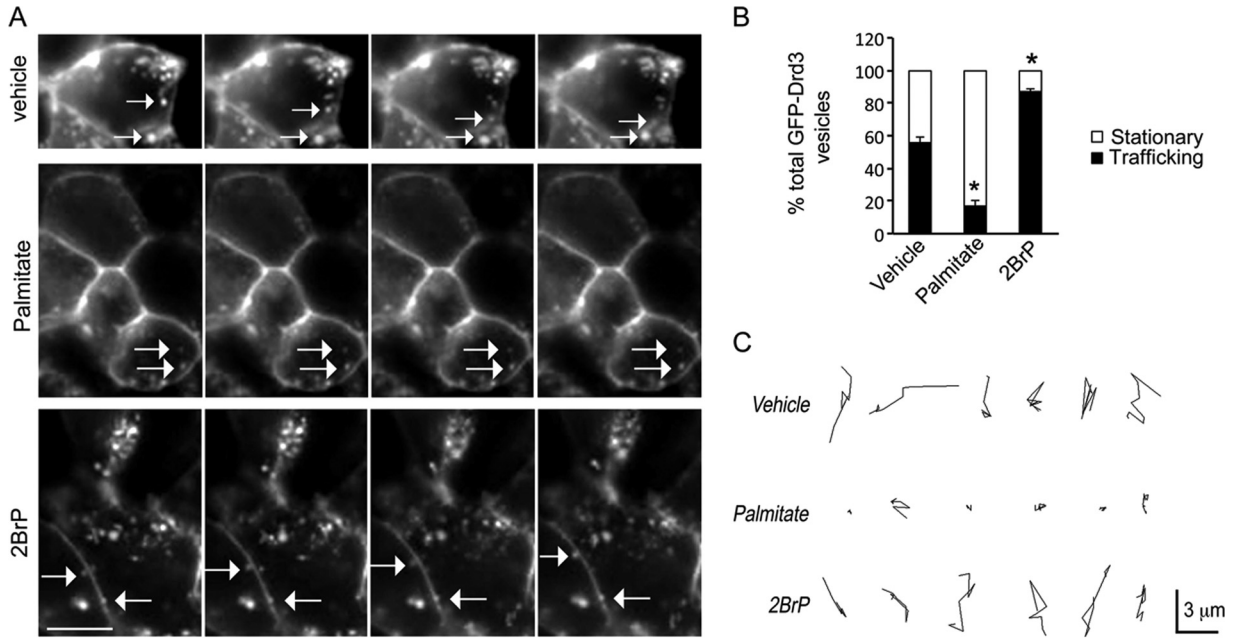

FIG 6 2BrP increased the motility of GFP-Drd3 cargo vesicles. (A) Effect of 20 μM palmitate or 20 μM 2BrP on the trafficking of GFP-Drd3 cargo vesicles in HEK293 cells cotransfected with GIPC1. Images were taken every 5 s. Scale bar, 4 μm. (B) Relative proportion of GFP-Drd3 vesicles that are stationary or trafficking. Means ± SEM for data collected from 20 cells per condition are shown (unpaired *t* test; $P < 0.0001$). (C) Representative tracks used by individual vesicles.

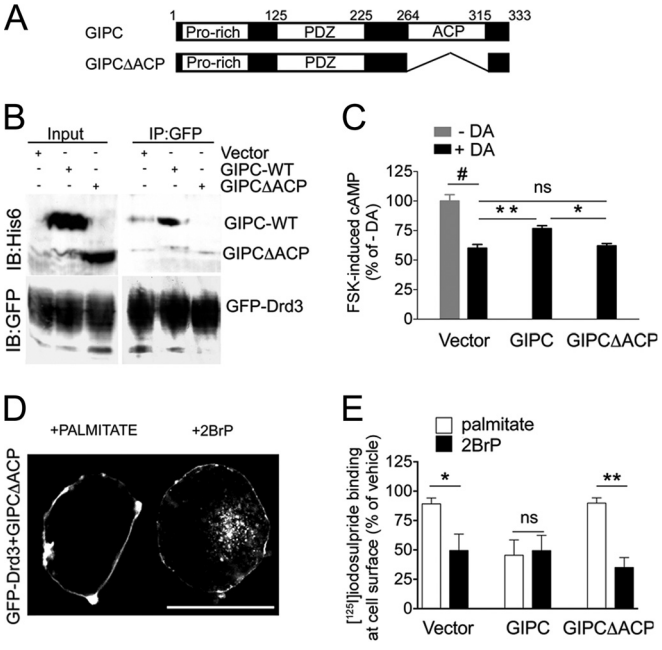

FIG 7 Description of a GIPC1 mutant that cannot bind to Drd3. (A) Schematic representation of GIPC1 and mutant lacking the ACP domain. (B) GIPC1ΔACP did not bind to GFP-Drd3, as shown by coimmunoprecipitation from lysates of HEK293 cells cotransfected with GFP-Drd3 and the GIPC1 construct. (C) Inhibition of cAMP accumulation by a 15-min stimulation with 0.1 μM DA in HEK293 cells cotransfected with GFP-Drd3 and GIPC1 or the control vector in the presence of 0.5 μM FSK. Means ± SEM of data from 3 independent experiments (unpaired *t* test; #, $P < 0.0001$; **, $P = 0.0034$; *, $P = 0.0221$). (D) Representative HEK293 cells cotransfected with GFP-Drd3 and GIPC1ΔACP after stimulation with 100 μM palmitate or 100 μM 2BrP overnight. Scale bar, 12 μm. (E) Effects of GIPC1ΔACP on the binding of 0.1 nM [^{125}I]iodosulpride to whole-cell preparations of HEK293 cells cotransfected with GFP-Drd3 and GIPC1 constructs. Means ± SEM of data from 4 experiments (unpaired *t* test; *, $P = 0.0294$; **, $P = 0.0047$).

dently of GIPC1 binding, we generated a Drd3 mutant that coimmunoprecipitated and colocalized with GIPC1 (Fig. 9A and C) but failed to be palmitoylated in HEK293 cells (Fig. 9B). This mutant, GFP-Drd3C/S, was not properly targeted to the plasma membrane of transfected HEK293 cells and failed to respond to pretreatment with 2-BrP (Fig. 9D and E), compared to the wild-type GFP-Drd3 (WT). Functionally, GFP-Drd3C/S failed to respond to dopamine in inhibiting the cAMP pathway, either with or without pretreatment with 2BrP (Fig. 9F). Yet, GFP-Drd3C/S fully responded to dopamine for inhibiting the phosphorylation of Akt and for activating the Erk pathway (Fig. 9G). Together, the results indicate that Drd3 palmitoylation is dispensable for Erk and Akt signaling but essential for the cAMP signaling route.

DISCUSSION

In this study, we extended the *in silico* modeling of the GIPC1-Drd2 interaction (10) to the cognate GIPC1-Drd3 interaction, as the template, and then validated the model in *in cellulo* experiments. Molecular dynamic (MD) simulations predicted that C-terminal palmitoylation of Drd3 would enhance the penetration of each residue of the C terminus, including the helix-8, into the membrane environment, thus reducing accessibility to interaction domains with intracellular proteins, notably, the PDZ domain of GIPC1, as proposed for the Drd2. *In cellulo* experiments confirmed the prediction, thereby providing a framework for understanding how reversible Drd3 palmitoylation controls dopamine signaling via the GIPC1 route. These findings could be significant for Drd3 pleiotropic functions in physiology and treatment with antipsychotic and anti-Parkinsonian drugs.

In two different cell lines, Drd3 was constitutively palmitoylated at multiple molecular mass isoforms between 40 and 55 kDa (65 and 80 kDa for GFP-Drd3) which are likely to correspond to intermediates of glycosylation, given that constitutive pal-

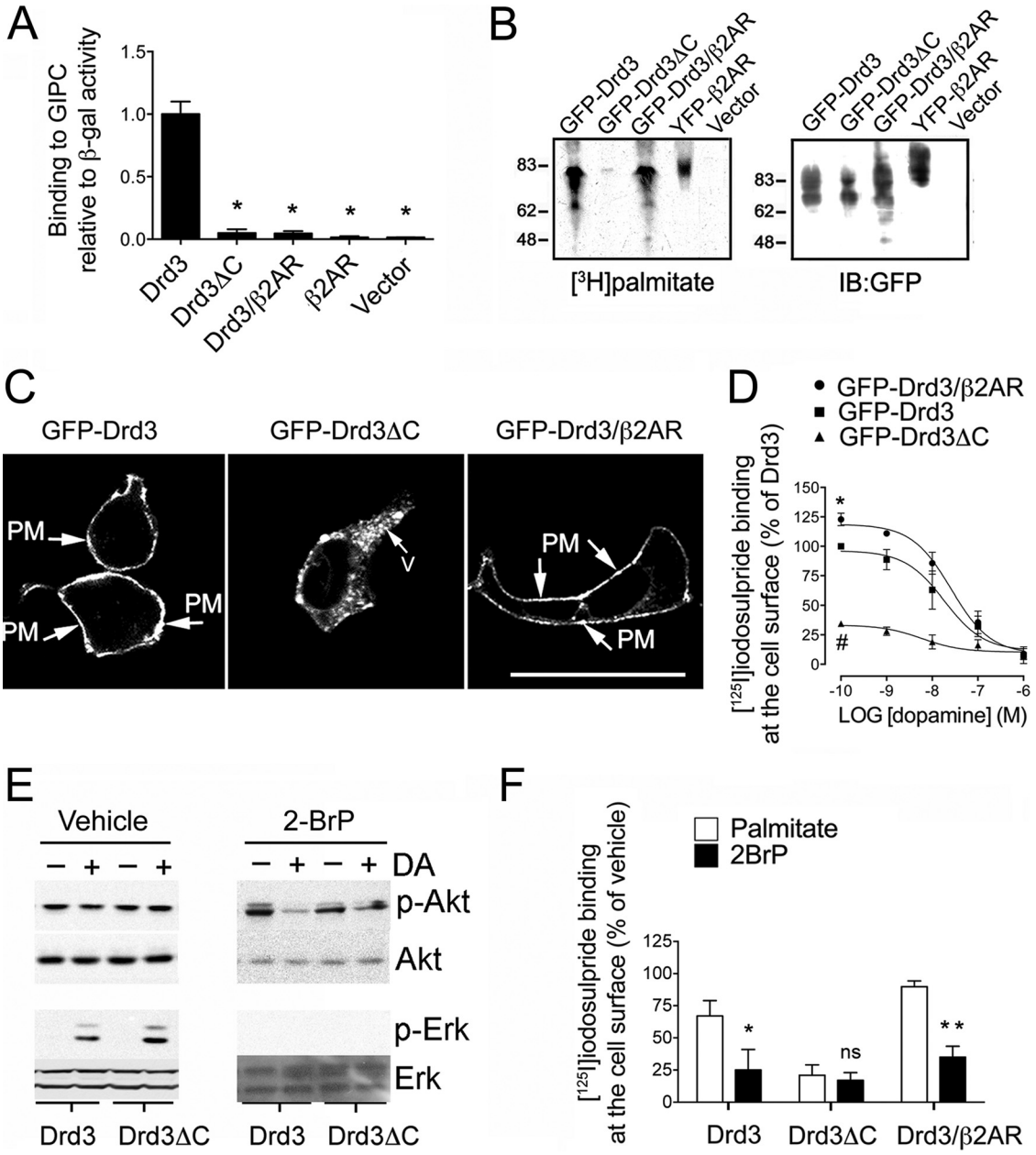

FIG 8 Description of a palmitoylated Drd3 mutant that cannot bind to GIPC1. (A) Binding of GIPC1 to Drd3 mutants monitored by β-galactosidase activity using ONPG as the substrate in yeast. The Drd3ΔC lacks the C-terminal cysteine residue, whereas the Drd3/β2AR chimera harbors the palmitoylation site of Drd3 and the C-terminal PDZ ligand of the β2AR. Means ± SEM of data collected from 3 independent experiments are shown (unpaired *t* test; *, $P < 0.01$). (B) Palmitoylation of GFP-Drd3 mutants in HEK293 cells. (C) Subcellular distribution of GFP-Drd3 mutants transfected in HEK293 cells. Scale bar, 20 μm. PM, plasma membrane. (D) Binding of [^{125}I]iodosulpride at the cell surface of HEK293 cells transfected with the GFP-Drd3 constructs in competition with increasing concentrations of dopamine. Means ± SEM of data collected from 3 independent experiments (unpaired *t* test; *, $P = 0.0017$ for WT versus Drd3/β2AR; #, $P < 0.0001$ for WT versus Drd3ΔC). (E) Effect of Drd3ΔC on Erk and Akt phosphorylations upon a 4-min stimulation with 0.1 μM DA in HEK293 cells pretreated with 50 μM 2-BrP or vehicle overnight. (F) Effect of 100 μM palmitate and 100 μM 2-BrP on [^{125}I]iodosulpride binding at the cell surface of HEK293 cells transfected with the indicated GFP-Drd3 constructs. Means ± SEM of data collected from 3 independent experiments (unpaired *t* test, vehicle versus 2-BrP; *, $P = 0.0313$; **, $P = 0.0054$).

mitoylation is an early posttranslational modification occurring in the ER and Golgi apparatus, where glycosylation occurs (62). Lack of Drd3 palmitoylation by nonselective pharmacological blockade with 2BrP or by targeted mutation of the C-terminal cysteine resulted in the accumulation of Drd3 in intracellular membrane compartments. Further experiments using an anterograde transport assay, whole-cell Drd3 radioligand binding, antibody feeding assay, and live imaging of Drd3 cargo vesicles consistently supported the idea that palmitoylation is required to target and stabilize Drd3 at the cell surface. The use of the chimeric Drd3/β2AR mutant and Drd3-C/S mutant was instrumental to demonstrate that Drd3 palmitoyl-

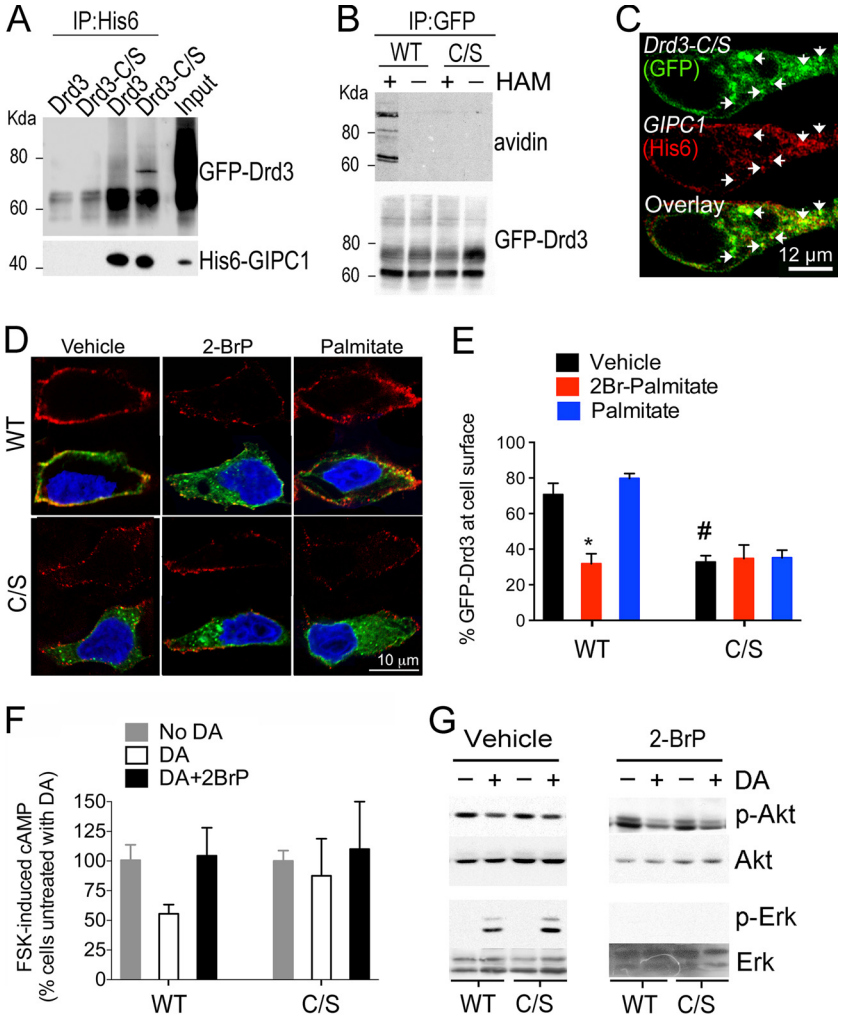

FIG 9 Description of a nonpalmitoylated Drd3 mutant that can bind to GIPC1. (A) Coimmunoprecipation of GIPC1 with GFP-Drd3 or GFP-Drd3C/S mutants from HEK293 transfected cells using 6×His antibodies. (B) Mutant GFP-Drd3C/S was not palmitoylated in HEK293 transfected cells compared to GFP-Drd3. Palmitoylation was measured using acyl-biotin exchange (see Materials and Methods). HAM, hydroxylamine. (C) The GFP-Drd3C/S mutant colocalized with GIPC1 in transfected HEK293 cells. (D) GFP antibody feeding assay on transfected HEK293 cells to label GFP-Drd3 and mutant GFP-Drd3C/S at the cell surface (red) compared to total GFP expression (green). The nuclei were labeled with Hoechst 33342 (blue). (E) Percentage of Drd3 at the cell surface. Means ± SEM of data from at least 10 cells per condition in 2 independent experiments are shown (unpaired *t* test; *, $P = 0.0003$; #, $P < 0.0001$). (F) Effect of Drd3C/S on the inhibition of cAMP accumulation by a 15-min stimulation with 0.1 μM DA in the presence of 0.5 μM FSK in HEK293 cells pretreated with 15 μM 2-BrP or vehicle overnight. Means ± SD ($n = 3$) are shown (unpaired *t* test; *, $P = 0.007$). (G) Effect of Drd3C/S on Erk and Akt phosphorylation upon a 4-min stimulation with 0.1 μM DA in HEK293 cells pretreated with 50 μM 2-BrP or vehicle overnight.

ation is essential for Drd3 presentation at the cell surface and that GIPC1 binding favors a vesicular distribution for Drd3. This is consistent with the physiological distribution of Drd3 and GIPC1 in the adult rat brain, as well as in embryo-derived cultured primary MSNs. Interestingly, palmitoylation decreased the motility of Drd3 cargo vesicles, perhaps by reducing access of Drd3 cargoes to cytoskeletal motor proteins for which GIPC1 is an established adaptor (39, 63, 64).

GIPC1 colocalized with Drd3 in vesicles and at the plasma membrane of HEK293 cells. Inhibition of cellular palmitoylation with 2BrP rearranged this colocalization, particularly in vesicles close to the cell surface and at the plasma membrane. Given that transfected GIPC1 decreased the levels of Drd3 palmitoylation, we anticipate that GIPC1 binds to depalmitoylated Drd3, as predicted for Drd2 in the *in silico* model. This is consistent with a competition at the Drd3 C terminus for overlapping consensus sites for palmitoylation and GIPC1 binding (Fig. 1A). This possibility is corroborated experimentally by the disruption of the interaction between GIPC1 and Drd3 with a nonpalmitoylated synthetic peptide mimetic of the Drd3 C terminus (21). In addition, molecular modeling predicts that helix-8 is not structurally changed much by palmitoylation but that it is more deeply inserted into the membrane environment. In contrast, a depalmitoylated C terminus is more exposed to the aqueous environment and presumably protein partners like GIPC1, thus reinforcing the opposition between the palmitoylation and GIPC interaction at Drd3. This may also be true for Drd2, as suggested by results of transfection experiments in primary MSNs (Fig. 4B) (10). The presence of an ACP domain in GIPC1 suggests a putative function in the

acylation of target PDZ cargoes (36). We found that the GIPC1 ACP domain contributed to the interaction with Drd3 in yeast and HEK293 cells. However, the exact role of the ACP domain has not been extensively studied and is beyond the scope of this study.

Palmitoylation is a reversible and dynamic process (22). It is thought that palmitoylation of GPCRs can sometimes be stable (e.g., 5-HT1a [65, 66]) or, most commonly, reversible (e.g., 5-HT4a and 5-HT7a [67, 68]), resulting in different loop conformations as the palmitate groups penetrate into the lipid bilayer, thereby changing GPCR dimerization and signaling properties (3, 12). Several studies reported distinct effects of ligand-induced activation on palmitoylation. For example, activation of the β2AR with isoproterenol did not change its palmitoylation rate (69). In contrast, increased turnover of palmitoylation was demonstrated at least for the CHRM2, AVPR2, and 5-HT4a receptors (67, 70, 71). These studies suggested that one possible role for palmitoylation is to change the turnover of target transmembrane proteins and thus their functional properties. An example of this phenomenon is the mannose-6-phosphate receptor, for which the half-life is 40 h when depalmitoylated and 2 h when palmitoylated (72). Consistently, overexpression of GIPC1 decreased Drd3 palmitoylation and Drd3 lysosomal degradation (21). Future experiments will determine if Drd3 undergoes cycles of palmitoylation and depalmitoylation during its lifetime. Such a dynamic process could facilitate the trafficking and signaling of depalmitoylated Drd3 cargoes by a GIPC1 signaling route.

Amid the complexity of dopamine signaling pathways (26, 73, 74), the cAMP pathway inhibited by Drd3 was most sensitive to GIPC1 and palmitoylation. Interestingly, the Erk pathway was sensitive to 2BrP but not to Drd3 mutations, indicating that cellular palmitoylation rather than Drd3 palmitoylation is involved in this process, as previously suggested in cancer cells (75). On the contrary, dopamine signaling via the Akt pathway required GIPC1 regardless of 2BrP treatment, given that Drd3ΔC failed to inhibit Akt phosphorylation by dopamine. This is corroborated by results in a previous study, indicating that the GIPC1 expression level can modulate Akt phosphorylation by bovine serum albumin (43).

In summary, GIPC1 competes with Drd3 palmitoylation, thereby impacting the presentation of the Drd3 at the plasma membrane, the access of extracellular ligands, and the dopaminergic signal transduction. Given the important role of Drd3 in the mode of action of antipsychotic drugs for treating schizophrenia (29), in the underlying mechanisms of levodopa-induced dyskinesia (31), and as a genetic predisposition factor in essential tremor (30), the GIPC1-palmitoylation switch of Drd3 provides novel mechanistic insights for manipulating dopaminergic signaling when it is impaired.

ACKNOWLEDGMENTS

The work was supported by the Fondation pour la Recherche Médicale, the Fondation de France, and the French Ministry of Research.

We thank M. Asari for figure editing.

M.A.-L., P.S., and F.J. conceived all experiments. O.S. and H.W. designed the computational experiments. M.A.-L. and F.J. collected biochemical data. M.A.-L. and M.C. produced time-lapse fluorescence imaging data. G.G. and A.B. did binding and cAMP experiments. O.S. performed *in silico* simulation studies. M.A.-L. and F.J. wrote the manuscript, with contributions from O.S., H.W., and P.S.

We declare no competing interests.

FUNDING INFORMATION

Fondation pour la recherche medicale provided funding to Pierre Sokoloff and Freddy Jeanneteau. French ministry of research provided funding to Freddy Jeanneteau. Fondation de France provided funding to Margarita Arango-Lievano and Freddy Jeanneteau.

REFERENCES

1. **Bockaert J, Marin P, Dumuis A, Fagni L.** 2003. The 'magic tail' of G protein-coupled receptors: an anchorage for functional protein networks. FEBS Lett **546:**65–72. http://dx.doi.org/10.1016/S0014-5793(03)00453-8.
2. **Dunn HA, Ferguson SS.** 2015. PDZ protein regulation of GPCR trafficking and signaling pathways. Mol Pharmacol **88:**624–639. http://dx.doi.org/10.1124/mol.115.098509.
3. **Qanbar R, Bouvier M.** 2003. Role of palmitoylation/depalmitoylation reactions in G-protein-coupled receptor function. Pharmacol Ther **97:**1–33. http://dx.doi.org/10.1016/S0163-7258(02)00300-5.
4. **Goddard AD, Watts A.** 2012. Regulation of G protein-coupled receptors by palmitoylation and cholesterol. BMC Biol **10:**27. http://dx.doi.org/10.1186/1741-7007-10-27.
5. **Oates J, Watts A.** 2011. Uncovering the intimate relationship between lipids, cholesterol and GPCR activation. Curr Opin Struct Biol **21:**802–807. http://dx.doi.org/10.1016/j.sbi.2011.09.007.
6. **Zheng H, Pearsall EA, Hurst DP, Zhang Y, Chu J, Zhou Y, Reggio PH, Loh HH, Law PY.** 2012. Palmitoylation and membrane cholesterol stabilize mu-opioid receptor homodimerization and G protein coupling. BMC Cell Biol **13:**6. http://dx.doi.org/10.1186/1471-2121-13-6.
7. **Palczewski K, Kumasaka T, Hori T, Behnke CA, Motoshima H, Fox BA, Le Trong I, Teller DC, Okada T, Stenkamp RE, Yamamoto M, Miyano M.** 2000. Crystal structure of rhodopsin: a G protein-coupled receptor. Science **289:**739–745. http://dx.doi.org/10.1126/science.289.5480.739.
8. **Scheerer P, Park JH, Hildebrand PW, Kim YJ, Krauss N, Choe HW, Hofmann KP, Ernst OP.** 2008. Crystal structure of opsin in its G-protein-interacting conformation. Nature **455:**497–502. http://dx.doi.org/10.1038/nature07330.
9. **Krishna AG, Menon ST, Terry TJ, Sakmar TP.** 2002. Evidence that helix 8 of rhodopsin acts as a membrane-dependent conformational switch. Biochemistry **41:**8298–8309. http://dx.doi.org/10.1021/bi025534m.
10. **Sensoy O, Weinstein H.** 2015. A mechanistic role of Helix 8 in GPCRs: computational modeling of the dopamine D2 receptor interaction with the GIPC1-PDZ-domain. Biochim Biophys Acta **1848:**976–983. http://dx.doi.org/10.1016/j.bbamem.2014.12.002.
11. **Ernst OP, Meyer CK, Marin EP, Henklein P, Fu WY, Sakmar TP, Hofmann KP.** 2000. Mutation of the fourth cytoplasmic loop of rhodopsin affects binding of transducin and peptides derived from the carboxyl-terminal sequences of transducin alpha and gamma subunits. J Biol Chem **275:**1937–1943. http://dx.doi.org/10.1074/jbc.275.3.1937.
12. **Cherezov V, Rosenbaum DM, Hanson MA, Rasmussen SG, Thian FS, Kobilka TS, Choi HJ, Kuhn P, Weis WI, Kobilka BK, Stevens RC.** 2007. High-resolution crystal structure of an engineered human β2-adrenergic G protein-coupled receptor. Science **318:**1258–1265. http://dx.doi.org/10.1126/science.1150577.
13. **Shan J, Khelashvili G, Mondal S, Mehler EL, Weinstein H.** 2012. Ligand-dependent conformations and dynamics of the serotonin 5-HT(2A) receptor determine its activation and membrane-driven oligomerization properties. PLoS Comput Biol **8:**e1002473. http://dx.doi.org/10.1371/journal.pcbi.1002473.
14. **Delos Santos NM, Gardner LA, White SW, Bahouth SW.** 2006. Characterization of the residues in helix 8 of the human β1-adrenergic receptor that are involved in coupling the receptor to G proteins. J Biol Chem **281:**12896–12907. http://dx.doi.org/10.1074/jbc.M508500200.
15. **Tetsuka M, Saito Y, Imai K, Doi H, Maruyama K.** 2004. The basic residues in the membrane-proximal C-terminal tail of the rat melanin-concentrating hormone receptor 1 are required for receptor function. Endocrinology **145:**3712–3723. http://dx.doi.org/10.1210/en.2003-1638.
16. **Kuwasako K, Hay DL, Nagata S, Murakami M, Kitamura K, Kato J.** 2013. Functions of third extracellular loop and helix 8 of family B GPCRs complexed with RAMPs and characteristics of their receptor trafficking. Curr Protein Peptide Sci **14:**416–428. http://dx.doi.org/10.2174/13892037113149990058.
17. **Jin H, Zastawny R, George SR, O'Dowd BF.** 1997. Elimination of palmitoylation sites in the human dopamine D1 receptor does not affect

receptor-G protein interaction. Eur J Pharmacol **324:**109–116. http://dx.doi.org/10.1016/S0014-2999(97)00059-9.
18. **Ng GY, O'Dowd BF, Caron M, Dennis M, Brann MR, George SR.** 1994. Phosphorylation and palmitoylation of the human D2L dopamine receptor in Sf9 cells. J Neurochem **63:**1589–1595.
19. **Chien EY, Liu W, Zhao Q, Katritch V, Han GW, Hanson MA, Shi L, Newman AH, Javitch JA, Cherezov V, Stevens RC.** 2010. Structure of the human dopamine D3 receptor in complex with a D2/D3 selective antagonist. Science **330:**1091–1095. http://dx.doi.org/10.1126/science.1197410.
20. **Ebersole B, Petko J, Woll M, Murakami S, Sokolina K, Wong V, Stagljar I, Luscher B, Levenson R.** 2015. Effect of C-terminal S-palmitoylation on D2 dopamine receptor trafficking and stability. PLoS One **10:**e0140661. http://dx.doi.org/10.1371/journal.pone.0140661.
21. **Jeanneteau F, Diaz J, Sokoloff P, Griffon N.** 2004. Interactions of GIPC with dopamine D2, D3 but not D4 receptors define a novel mode of regulation of G protein-coupled receptors. Mol Biol Cell **15:**696–705.
22. **Fukata Y, Fukata M.** 2010. Protein palmitoylation in neuronal development and synaptic plasticity. Nat Rev Neurosci **11:**161–175. http://dx.doi.org/10.1038/nrn2788.
23. **Blanpain C, Wittamer V, Vanderwinden JM, Boom A, Renneboog B, Lee B, Le Poul E, El Asmar L, Govaerts C, Vassart G, Doms RW, Parmentier M.** 2001. Palmitoylation of CCR5 is critical for receptor trafficking and efficient activation of intracellular signaling pathways. J Biol Chem **276:**23795–23804. http://dx.doi.org/10.1074/jbc.M100583200.
24. **Dunphy JT, Greentree WK, Manahan CL, Linder ME.** 1996. G-protein palmitoyltransferase activity is enriched in plasma membranes. J Biol Chem **271:**7154–7159. http://dx.doi.org/10.1074/jbc.271.12.7154.
25. **Berthet A, Bezard E.** 2009. Dopamine receptors and L-dopa-induced dyskinesia. Parkinsonism Relat Disord **15**(Suppl 4):S8–12. http://dx.doi.org/10.1016/S1353-8020(09)70827-2.
26. **Beaulieu JM, Gainetdinov RR.** 2011. The physiology, signaling, and pharmacology of dopamine receptors. Pharmacol Rev **63:**182–217. http://dx.doi.org/10.1124/pr.110.002642.
27. **Deng H, Le W, Jankovic J.** 2007. Genetics of essential tremor. Brain **130:**1456–1464. http://dx.doi.org/10.1093/brain/awm018.
28. **Joyce JN, Millan MJ.** 2007. Dopamine D3 receptor agonists for protection and repair in Parkinson's disease. Curr Opin Pharmacol **7:**100–105. http://dx.doi.org/10.1016/j.coph.2006.11.004.
29. **Sokoloff P, Leriche L, Diaz J, Louvel J, Pumain R.** 2013. Direct and indirect interactions of the dopamine D(3) receptor with glutamate pathways: implications for the treatment of schizophrenia. Naunyn-Schmiedebergs Arch Pharmacol **386:**107–124. http://dx.doi.org/10.1007/s00210-012-0797-0.
30. **Jeanneteau F, Funalot B, Jankovic J, Deng H, Lagarde JP, Lucotte G, Sokoloff P.** 2006. A functional variant of the dopamine D3 receptor is associated with risk and age-at-onset of essential tremor. Proc Natl Acad Sci U S A **103:**10753–10758. http://dx.doi.org/10.1073/pnas.0508189103.
31. **Bezard E, Ferry S, Mach U, Stark H, Leriche L, Boraud T, Gross C, Sokoloff P.** 2003. Attenuation of levodopa-induced dyskinesia by normalizing dopamine D3 receptor function. Nat Med **9:**762–767. http://dx.doi.org/10.1038/nm875.
32. **Missale C, Nash SR, Robinson SW, Jaber M, Caron MG.** 1998. Dopamine receptors: from structure to function. Physiol Rev **78:**189–225.
33. **Sokoloff P, Diaz J, Le Foll B, Guillin O, Leriche L, Bezard E, Gross C.** 2006. The dopamine D3 receptor: a therapeutic target for the treatment of neuropsychiatric disorders. CNS Neurol Disord Drug Targets **5:**25–43. http://dx.doi.org/10.2174/187152706784111551.
34. **Griffon N, Pilon C, Sautel F, Schwartz JC, Sokoloff P.** 1997. Two intracellular signaling pathways for the dopamine D3 receptor: opposite and synergistic interactions with cyclic AMP. J Neurochem **68:**1–9.
35. **Rasolonjanahary R, Gerard C, Dufour MN, Homburger V, Enjalbert A, Guillon G.** 2002. Evidence for a direct negative coupling between dopamine-D2 receptors and PLC by heterotrimeric Gi1/2 proteins in rat anterior pituitary cell membranes. Endocrinology **143:**747–754. http://dx.doi.org/10.1210/endo.143.3.8697.
36. **De Vries L, Lou X, Zhao G, Zheng B, Farquhar MG.** 1998. GIPC, a PDZ domain containing protein, interacts specifically with the C terminus of RGS-GAIP. Proc Natl Acad Sci U S A **95:**12340–12345. http://dx.doi.org/10.1073/pnas.95.21.12340.
37. **Hu LA, Chen W, Martin NP, Whalen EJ, Premont RT, Lefkowitz RJ.** 2003. GIPC interacts with the β1-adrenergic receptor and regulates β1-adrenergic receptor-mediated ERK activation. J Biol Chem **278:**26295–26301. http://dx.doi.org/10.1074/jbc.M212352200.
38. **Cai H, Reed RR.** 1999. Cloning and characterization of neuropilin-1-interacting protein: a PSD-95/Dlg/ZO-1 domain-containing protein that interacts with the cytoplasmic domain of neuropilin-1. J Neurosci **19:**6519–6527.
39. **Bunn RC, Jensen MA, Reed BC.** 1999. Protein interactions with the glucose transporter binding protein GLUT1CBP that provide a link between GLUT1 and the cytoskeleton. Mol Biol Cell **10:**819–832. http://dx.doi.org/10.1091/mbc.10.4.819.
40. **Lou X, Yano H, Lee F, Chao MV, Farquhar MG.** 2001. GIPC and GAIP form a complex with TrkA: a putative link between G protein and receptor tyrosine kinase pathways. Mol Biol Cell **12:**615–627. http://dx.doi.org/10.1091/mbc.12.3.615.
41. **Booth RA, Cummings C, Tiberi M, Liu XJ.** 2002. GIPC participates in G protein signaling downstream of insulin-like growth factor 1 receptor. J Biol Chem **277:**6719–6725. http://dx.doi.org/10.1074/jbc.M108033200.
42. **Blobe GC, Liu X, Fang SJ, How T, Lodish HF.** 2001. A novel mechanism for regulating transforming growth factor beta (TGF-beta) signaling. Functional modulation of type III TGF-beta receptor expression through interaction with the PDZ domain protein, GIPC. J Biol Chem **276:**39608–39617. http://dx.doi.org/10.1074/jbc.M106831200.
43. **Varsano T, Taupin V, Guo L, Baterina OY, Jr, Farquhar MG.** 2012. The PDZ protein GIPC regulates trafficking of the LPA1 receptor from APPL signaling endosomes and attenuates the cell's response to LPA. PLoS One **7:**e49227. http://dx.doi.org/10.1371/journal.pone.0049227.
44. **Beld J, Finzel K, Burkart MD.** 2014. Versatility of acyl-acyl carrier protein synthetases. Chem Biol **21:**1293–1299. http://dx.doi.org/10.1016/j.chembiol.2014.08.015.
45. **Heath RJ, Rock CO.** 1996. Regulation of fatty acid elongation and initiation by acyl-acyl carrier protein in Escherichia coli. J Biol Chem **271:**1833–1836. http://dx.doi.org/10.1074/jbc.271.4.1833.
46. **Othman A, Lazarus C, Fraser T, Stobart K.** 2000. Cloning of a palmitoyl-acyl carrier protein thioesterase from oil palm. Biochem Soc Trans **28:**619–622. http://dx.doi.org/10.1042/bst0280619.
47. **Phillips JC, Braun R, Wang W, Gumbart J, Tajkhorshid E, Villa E, Chipot C, Skeel RD, Kale L, Schulten K.** 2005. Scalable molecular dynamics with NAMD. J Comput Chem **26:**1781–1802. http://dx.doi.org/10.1002/jcc.20289.
48. **Marrink SJ, Risselada HJ, Yefimov S, Tieleman DP, de Vries AH.** 2007. The MARTINI force field: coarse grained model for biomolecular simulations. J Phys Chem B **111:**7812–7824. http://dx.doi.org/10.1021/jp071097f.
49. **Cerutti DS, Duke RE, Darden TA, Lybrand TP.** 2009. Staggered Mesh Ewald: an extension of the smooth particle-mesh Ewald method adding great versatility. J Chem Theory Comput **5:**2322. http://dx.doi.org/10.1021/ct9001015.
50. **Berendsen HJC, Postma JPM, van Gunsteren WF, DiNola A, Haak JR.** 1984. Molecular dynamics with coupling to an external bath. J Chem Phys **81:**3684–3690. http://dx.doi.org/10.1063/1.448118.
51. **Hyvönen MT, Kovanen PT.** 2003. Molecular dynamics simulation of sphingomyelin bilayer. J Phys Chem B **107:** 9102–9108. http://dx.doi.org/10.1021/jp035319v.
52. **Lim JB, Rogaski B, Klauda JB.** 2012. Update of the cholesterol force field parameters in CHARMM. J Phys Chem B **116:**203–210. http://dx.doi.org/10.1021/jp207925m.
53. **Heinig M, Frishman D.** 2004. STRIDE: a web server for secondary structure assignment from known atomic coordinates of proteins. Nucleic Acids Res **32:**W500–W502. http://dx.doi.org/10.1093/nar/gkh429.
54. **Weill C, Ilien B, Goeldner M, Galzi JL.** 1999. Fluorescent muscarinic EGFP-hM1 chimeric receptors: design, ligand binding and functional properties. J Receptor Signal Transduct Res **19:**423–436. http://dx.doi.org/10.3109/10799899909036662.
55. **Diaz J, Pilon C, Le Foll B, Gros C, Triller A, Schwartz JC, Sokoloff P.** 2000. Dopamine D3 receptors expressed by all mesencephalic dopamine neurons. J Neurosci **20:**8677–8684.
56. **Brigidi GS, Bamji SX.** 28 February 2013. Detection of protein palmitoylation in cultured hippocampal neurons by immunoprecipitation and acyl-biotin exchange (ABE). J Visual Exp http://dx.doi.org/10.3971/50031.
57. **Wan J, Roth AF, Bailey AO, Davis NG.** 2007. Palmitoylated proteins: purification and identification. Nat Protoc **2:**1573–1584. http://dx.doi.org/10.1038/nprot.2007.225.
58. **Sokoloff P, Levesque D, Martres MP, Lannfelt L, Diaz G, Pilon C, Schwartz JC.** 1992. The dopamine D3 receptor as a key target for anti-

psychotics. Clin Neuropharmacol **15**(Suppl 1)**:**456A–457A. http://dx.doi.org/10.1097/00002826-199201001-00238.
59. **Nuoffer C, Davidson HW, Matteson J, Meinkoth J, Balch WE.** 1994. A GDP-bound of rab1 inhibits protein export from the endoplasmic reticulum and transport between Golgi compartments. J Cell Biol **125:**225–237. http://dx.doi.org/10.1083/jcb.125.2.225.
60. **Davda D, El Azzouny MA, Tom CT, Hernandez JL, Majmudar JD, Kennedy RT, Martin BR.** 2013. Profiling targets of the irreversible palmitoylation inhibitor 2-bromopalmitate. ACS Chem Biol **8:**1912–1917. http://dx.doi.org/10.1021/cb400380s.
61. **Jennings BC, Nadolski MJ, Ling Y, Baker MB, Harrison ML, Deschenes RJ, Linder ME.** 2009. 2-Bromopalmitate and 2-(2-hydroxy-5-nitrobenzylidene)-benzo[b]thiophen-3-one inhibit DHHC-mediated palmitoylation in vitro. J Lipid Res **50:**233–242.
62. **Grunewald S, Haase W, Reilander H, Michel H.** 1996. Glycosylation, palmitoylation, and localization of the human D2S receptor in baculovirus-infected insect cells. Biochemistry **35:**15149–15161. http://dx.doi.org/10.1021/bi9607564.
63. **Valdembri D, Caswell PT, Anderson KI, Schwarz JP, Konig I, Astanina E, Caccavari F, Norman JC, Humphries MJ, Bussolino F, Serini G.** 2009. Neuropilin-1/GIPC1 signaling regulates α5β1 integrin traffic and function in endothelial cells. PLoS Biol **7:**e25. http://dx.doi.org/10.1371/journal.pbio.1000025.
64. **Yano H, Ninan I, Zhang H, Milner TA, Arancio O, Chao MV.** 2006. BDNF-mediated neurotransmission relies upon a myosin VI motor complex. Nat Neurosci **9:**1009–1018. http://dx.doi.org/10.1038/nn1730.
65. **Papoucheva E, Dumuis A, Sebben M, Richter DW, Ponimaskin EG.** 2004. The 5-hydroxytryptamine(1A) receptor is stably palmitoylated, and acylation is critical for communication of receptor with Gi protein. J Biol Chem **279:**3280–3291. http://dx.doi.org/10.1074/jbc.M308177200.
66. **Gorinski N, Ponimaskin E.** 2013. Palmitoylation of serotonin receptors. Biochem Soc Trans **41:**89–94. http://dx.doi.org/10.1042/BST20120235.
67. **Ponimaskin EG, Schmidt MF, Heine M, Bickmeyer U, Richter DW.** 2001. 5-Hydroxytryptamine 4(a) receptor expressed in Sf9 cells is palmitoylated in an agonist-dependent manner. Biochem J **353:**627–634. http://dx.doi.org/10.1042/bj3530627.
68. **Kvachnina E, Dumuis A, Wlodarczyk J, Renner U, Cochet M, Richter DW, Ponimaskin E.** 2009. Constitutive Gs-mediated, but not G12-mediated, activity of the 5-hydroxytryptamine 5-HT7(a) receptor is modulated by the palmitoylation of its C-terminal domain. Biochim Biophys Acta **1793:**1646–1655. http://dx.doi.org/10.1016/j.bbamcr.2009.08.008.
69. **Trester-Zedlitz M, Burlingame A, Kobilka B, von Zastrow M.** 2005. Mass spectrometric analysis of agonist effects on posttranslational modifications of the beta-2 adrenoceptor in mammalian cells. Biochemistry **44:**6133–6143. http://dx.doi.org/10.1021/bi0475469.
70. **Charest PG, Bouvier M.** 2003. Palmitoylation of the V2 vasopressin receptor carboxyl tail enhances beta-arrestin recruitment leading to efficient receptor endocytosis and ERK1/2 activation. J Biol Chem **278:**41541–41551. http://dx.doi.org/10.1074/jbc.M306589200.
71. **Hayashi MK, Haga T.** 1997. Palmitoylation of muscarinic acetylcholine receptor m2 subtypes: reduction in their ability to activate G proteins by mutation of a putative palmitoylation site, cysteine 457, in the carboxyl-terminal tail. Arch Biochem Biophys **340:**376–382. http://dx.doi.org/10.1006/abbi.1997.9906.
72. **Schweizer A, Kornfeld S, Rohrer J.** 1996. Cysteine 34 of the cytoplasmic tail of the cation-dependent mannose 6-phosphate receptor is reversibly palmitoylated and required for normal trafficking and lysosomal enzyme sorting. J Cell Biol **132:**577–584. http://dx.doi.org/10.1083/jcb.132.4.577.
73. **Beaulieu JM, Sotnikova TD, Yao WD, Kockeritz L, Woodgett JR, Gainetdinov RR, Caron MG.** 2004. Lithium antagonizes dopamine-dependent behaviors mediated by an AKT/glycogen synthase kinase 3 signaling cascade. Proc Natl Acad Sci U S A **101:**5099–5104. http://dx.doi.org/10.1073/pnas.0307921101.
74. **Beaulieu JM, Tirotta E, Sotnikova TD, Masri B, Salahpour A, Gainetdinov RR, Borrelli E, Caron MG.** 2007. Regulation of Akt signaling by D2 and D3 dopamine receptors in vivo. J Neurosci **27:**881–885. http://dx.doi.org/10.1523/JNEUROSCI.5074-06.2007.
75. **Heakal Y, Woll MP, Fox T, Seaton K, Levenson R, Kester M.** 2011. Neurotensin receptor-1 inducible palmitoylation is required for efficient receptor-mediated mitogenic-signaling within structured membrane microdomains. Cancer Biol Ther **12:**427–435. http://dx.doi.org/10.4161/cbt.12.5.15984.